Propagation and Dissipation of Ion Cyclotron Waves in the Auroral Ionosphere

Jay R. Johnson
C. Z. Cheng
Princeton Plasma Physics Laboratory

The primary focus of this research is to develop a model for understanding plasma and field properties in downward auroral current regions. In these regions, upgoing electron beams and heated ion populations are commonly observed. Observations of particle distributions in this region are also consistent with a downward pointing parallel electric field. The FAST satellite typically detects broadband electromagnetic wave activity near the ion cyclotron frequency over the range 4Hz-20kHz in downward current regions and there is evidence for wave energy absorption near the ion cyclotron frequency and its harmonics. It is of interest to understand the relationship between the particle populations and the concomitant waves. The energy flow carried by the Poynting flux of the waves is sufficient to explain the ion outflows in many cases. Moreover, the statistical study of Andre [Ion Energization Mechanisms at 1700 km in the auroral region, J. Geophys. Res., 4199, 1998] demonstrated that most ion heating events in the auroral region could be attributed to ion cyclotron waves.

Strong electron beams are one of many sources of free energy which can excite waves in the ion cyclotron frequency range. Those waves propagate into the ionosphere and where they dissipate and transfer wave energy to particle acceleration. Dissipation of wave energy leads to ion heating through collisions and/or ion cyclotron heating. As a result of the heating, ions flow out along field lines leading to modifications in the background plasma and electric field. These plasma changes feed back on the ion cyclotron instability and wave propagation. The goal of this work is to understand the long-time behavior of these regions considering the wave-particle feedback.

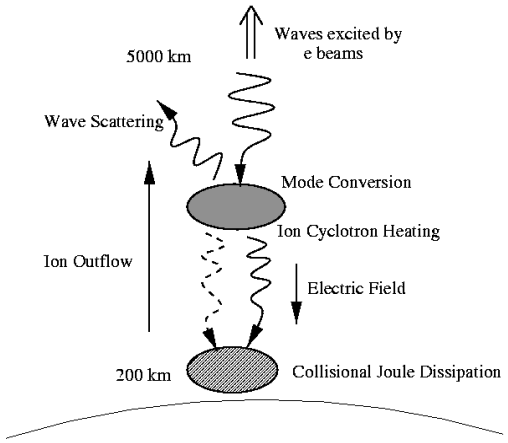

Figure 1. Electron beams accelerated by downward pointing electric field excite electromagnetic ion cyclotron waves. These waves are guided along field lines to a heavy ion resonance where wave energy scatters. Part of the wave energy is absorbed, but part is transmitted to the ionosphere where collisional heating of ions occurs. The dissipation leads to ion heating and ion outflows which modify the background plasma.

Wave Propagation Model

The first phase of this project is understand excitation and propagation and to identify how wave energy is transferred to ions in the ionosphere. Figure 1 illustrates the physical processes. Waves with frequency near the proton cyclotron frequency are excited in the auroral acceleration region (5000 km above the Earth's surface). The waves propagate into the topside ionosphere (because they have field aligned group velocity) where they encounter heavy ion resonances (helium and oxygen) in the increased magnetic field. The waves scatter off the resonant layer, but some wave energy is absorbed and some wave energy is transmitted to the ionosphere. In the collisional ionosphere, the waves may also be absorbed by ions. The remaining wave power is reflected off the ionosphere and may be efficiently absorbed at the heavy ion resonance. Heating of ions leads to outflows and modification of the parallel electric field.

For a wave propagation model we solve:

$$\nabla^2 \mathbf{E} - \nabla(\nabla \cdot \mathbf{E}) + \frac{\omega^2}{c^2} \mathbf{å}(s) \cdot E = 0$$

$$\mathbf{å}(s) = S(\mathbf{I} - \mathbf{bb}) - iD(\mathbf{e}_1 \mathbf{b} \times \mathbf{e}_2 - \mathbf{b} \times \mathbf{e}_1 \mathbf{e}_1) + P\mathbf{bb}$$

$$S = 1 - \sum_j \frac{\omega_{pj}^2 (\omega + i\nu_j)}{\omega[(\omega + i\nu_j)^2 - \Omega_j^2]}$$

$$D = 1 - \sum_j \frac{\omega_{pj}^2 \Omega_j}{\omega[(\omega + i\nu_j)^2 - \Omega_j^2]}$$

$$P = 1 - \sum_j \frac{\omega_{pj}^2}{\omega(\omega + i\nu_j)}$$

We take a collisional model and plasma profile from Banks and Kokarts [1973] and Knudsen et al., [1992]. The equations are solved in the vertical direction, z, with a variable choice of $k_\perp$. The boundary condition imposed at the ground is that the earth is a perfect conductor. At the upper boundary correcponding to FAST altitudes, the solutions are matched to WKB solutions.

The equations are solved in the complex plane along a contour that avoids the resonances. Four linearly independent solutions are obtained from which any wave scattering problem may be obtained by matrix manipulation. We employ a box method [Zwillinger, 1989] to obtain the numerical solutions and overcome the stiff equations. By requiring boundary conditions on both sides of the domain be satisfied, the numerical technique overcomes the stiffness.

In Figure 2 we show solutions of the electric fields as a function of altitude. In the electric field, it is easy to see that where the wave encounters the helium layer, there is an abrupt change in the character of the electric field which corresponds with helium heating. Lower in the ionosphere the ratio of E/B becomes larger due to changes in the Alfven velocity. The wave polarization chanes from mixed polarization to nearly right hand polarization indicating strong coupling between the compressional and transverse modes in the topside ionosphere.

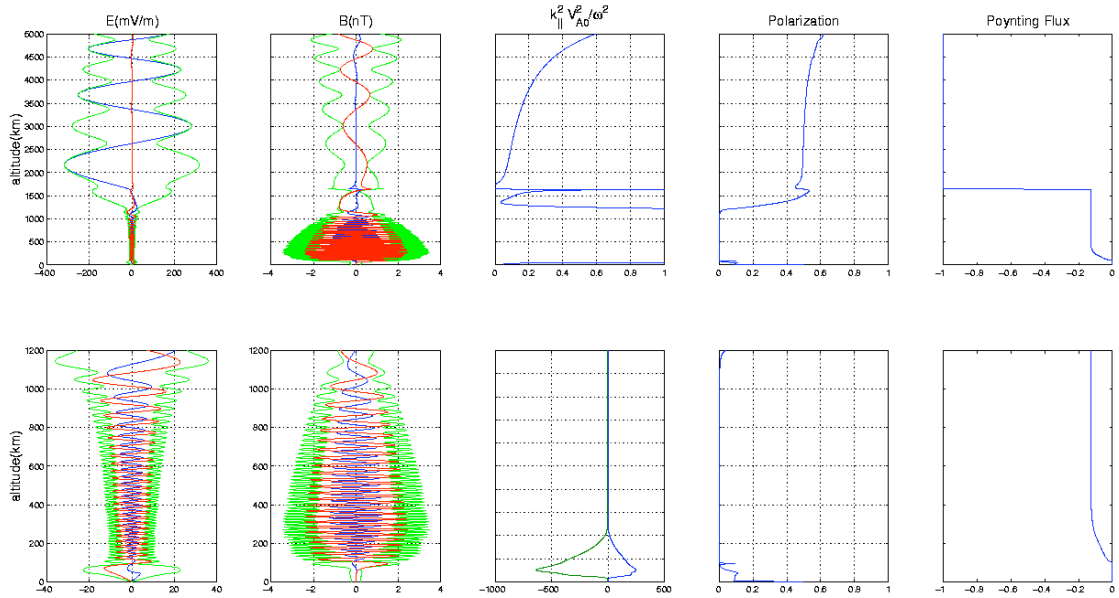

Fig 2 Solutions of the low frequency electromagnetic wave equations for waves excited in the auroral acceleration region. Plotted from left to right are: electric field, magnetic field, local wavevector, polarization, and Poynting flux as a function of altitude. The upper panels show the entire region from the auroral acceleration region to earth. The lower panel expands the solution in the ionosphere. Note especially that Poynting flux is lost near the He^+ resonance and in the ionosphere. For these solutions, the wave frequency is 128 Hz, oxygen and hydrogen each comprise 5% of the plasma concentration in the auroral acceleration region and the wave normal angle in the auroral acceleration region is 60°

Two particular scientific points of interest are apparent. First, we have provided theoretical evidence that high-frequency ion cyclotron waves (which commonly are observed modulating the aurora) could be detected on the ground, as shown in Fig.3(b). This finding is suggestive that modulations of optical aurora and/or electromagnetic rocket observations could be correlated with high-frequency ground based magnetometer measurements.

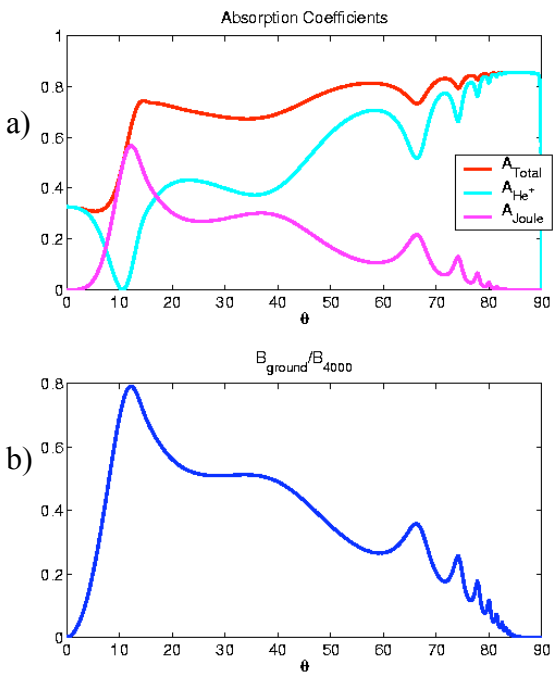

Fig 3. (a) Absorption coefficients as a function of angle between the wavevector and magnetic field direction in the auroral acceleration region. Note that Joule absorption and ion cyclotron resonant absorption both play an important role. Joule dissipation is large because the wave reaches the ionosphere as confirmed in panel (b). In panel (b) we compare the magnetic field wave amplitude at the ground with the amplitude in the source region. The results demonstrate that ion cyclotron waves with wave normal angle less than 85° can reach the ground with substantial amplitude. For both figures, the wave frequency is 128 Hz and the concentrations of oxygen and helium in the auroral acceleration region are 5%.

Such information would be useful for understanding wave propagation and absorption in the collisional ionosphere as well as heating of ionospheric ions through Joule dissipation.

Second, this work addresses one of the outstanding questions raised in the work of *Lund and LaBelle, [1997]*: "Can the beam-generated instabilities based on local plasma theory in the auroral acceleration region (5000 km) provide a source for ion cyclotron waves observed at rocket altitudes (400 km)?" To address this issue, we examined ion cyclotron wave propagation from the auroral acceleration region to the ionosphere using a realistic collisional model for the ionosphere. We found that ion cyclotron waves that are excited with wavenormal angle less than 85° may reach rocket altitudes (as shown in Fig. 3). This result is in contrast to the ray-tracing result for wave propagation that predicted only parallel propagating waves could reach rocket altitude in contrast with the observations. The underlying physical reason that the oblique waves could reach ionospheric altitude is because of a mode conversion process which is beyond the scope of ray-tracing. Morover, the mode conversion process also causes the H^+ ion cyclotron waves to have more spatial spread than the O^+ ion cyclotron waves consistent with observation.

However, this result has also raised a number of additional scientific issues. While there are many mechanisms for ion cyclotron wave generation that would be able to generate more field aligned waves, electron beam generated instabilities often have growth rates that peak around 85°, which is around the limit of the transmission window. Therefore, it is possible that other instabiltity mechanisms related to background distribution could excite waves with less oblique wavevector.

Particle Heating

Having established that ion cyclotron waves excited in the auroral acceleration region could propagate to the ionosphere and the ground, it is natural to consider their effect on particle energization. Because the magnetic field increases as the waves propagate toward the ground, the waves can interact with heavy ions through the ion cyclotron resonance. The waves can also interact with ions through ionospheric collisions. The wave solutions are useful for trying to understand wave and particle observations of satellites in the auroral region.

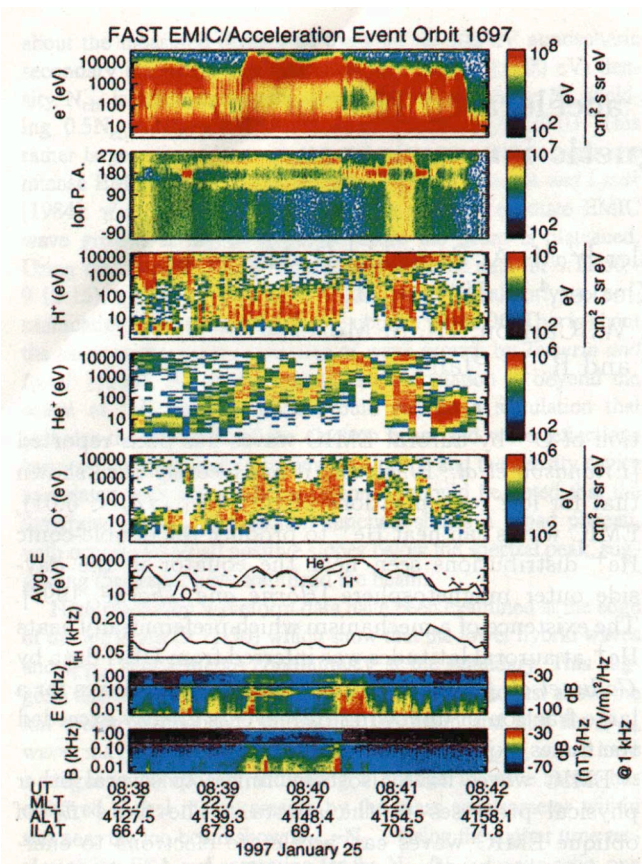

Figure 4. The FAST satellite detects an ion heating event showing preferential heating of helium ions in concert with electromagnetic ion cyclotron waves. Figure taken from Lund et al., GRL, 1998.

The FAST satellite frequently detects preferential heating of helium over oxygen and hydrogen. This observation is particularly interesting because typical heuristic heating rates based on quasilinear theory for ion cyclotron heating predict that the heating rate varies as $m^{\alpha-1}$ where m is the mass and α is spectral index of the the wave spectral density ($E^2 \sim f^{-\alpha}$). The best fit for α is usually larger than unity; therefore, a broadband heating rate would be more efficient for ions with larger mass (e.g. oxygen heating should be more efficient than helium heating). On the other hand, the observation shown in Figure 1 is typical and shows a preference for heating due to lighter mass. Lund et al., JASTP, 1999 suggest that over 80% of cases show preferential heating of helium over oxygen.

In obtaining the full wave solutions for ion cyclotron wave propagation, we have found that there is a strong dependence of the ion heating rate on minor species density and altitude related to wave propagation characteristics of the wave. In Figure 2, we show the absorption coefficients as a function of frequency and minor species concentration. The four panels show: (a) the total absorption, (b) the absorption at the helium resonance, (c) absorption at the oxygen resonance, and (d) absorption in the ionosphere. The wavevector for this plot was taken at 70 degrees and is typical for oblique propagation.

.

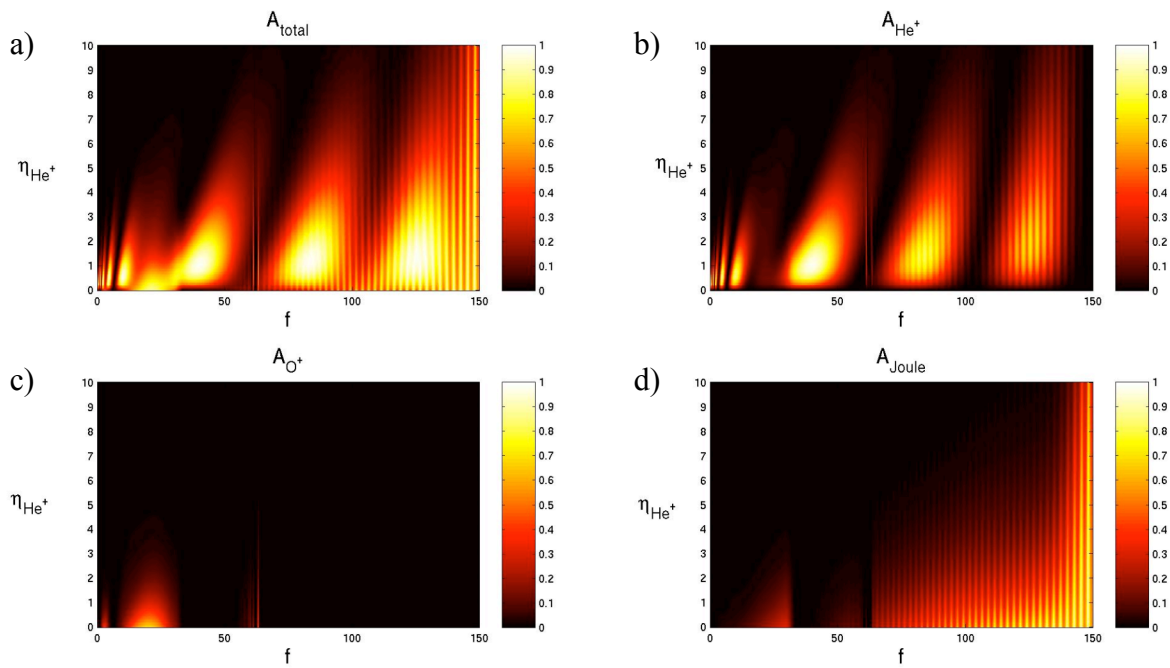

Figure 5. *Absorption coefficients are shown as a function of helium concentration (in percentage) and frequency, f. The four panels show: (a) the total absorption, (b) the absorption at the helium resonance, (c) absorption at the oxygen resonance, and (d) absorption in the ionosphere. Note that the most efficient wave absorption in the frequency range 50Hz –100Hz is at the helium resonance leading to efficient heating of helium. Oxygen ions are heated by the low-frequency portion of the wave spectrum when helium concentrations are below a few percent. The modulations in the absorption coefficients result from an ionospheric resonantor and are most pronounced at high frequency when Joule dissipation is large.*

Note that for a typical wave spectrum in the auroral region, the waves would heat helium more efficiently than oxygen. There are two modulations in the absorption coefficients. The large-scale modulation is due to reflection of the ion cyclotron waves from the ionosphere. Absorption is minimum if the reflected wave cancels the downcoming wave at the cyclotron resonance. The small-scale modulations result from coupling to the ionospheric resonantor and do not appear if the F region is removed from the model ionosphere.

A number of important conclusions should be drawn from this result. First, the wave absorption is strongly dependent on altitude and should lead to local pockets of ion heating. Second, the wave absorption is strongly dependent on minority species concentration because it affects wave propagation. However, the minority concentration will be modified if significant heating occurs. This means that there should be a significant feedback coupling the downcoming ion cyclotron

waves and the background ionospheric ion profiles with significant changes in the heating rates as a function of altitude dependent on the evolution of the background.

An Ionospheric Resonantor

In our previous report, we suggested that waves that reach the ionosphere interact with the F-region leading to fine scale absorption patterns as a function of frequency and wavelength. This phenomenon is shown in Figure 5 which shows the dependence of the absorption coefficient on frequency and the angle, θ, between the wavevector and magnetic field of the wave at the satellite location (4000 km). For parallel propagation, it is clear that there is a fine-scale frequency structure with roughly a 2-3 Hz structure. For larger angle of propagation, the frequency of the structures shifts upward. This upshift suggests that there is coupling of the downgoing ICW wave to a fast compressional wave.

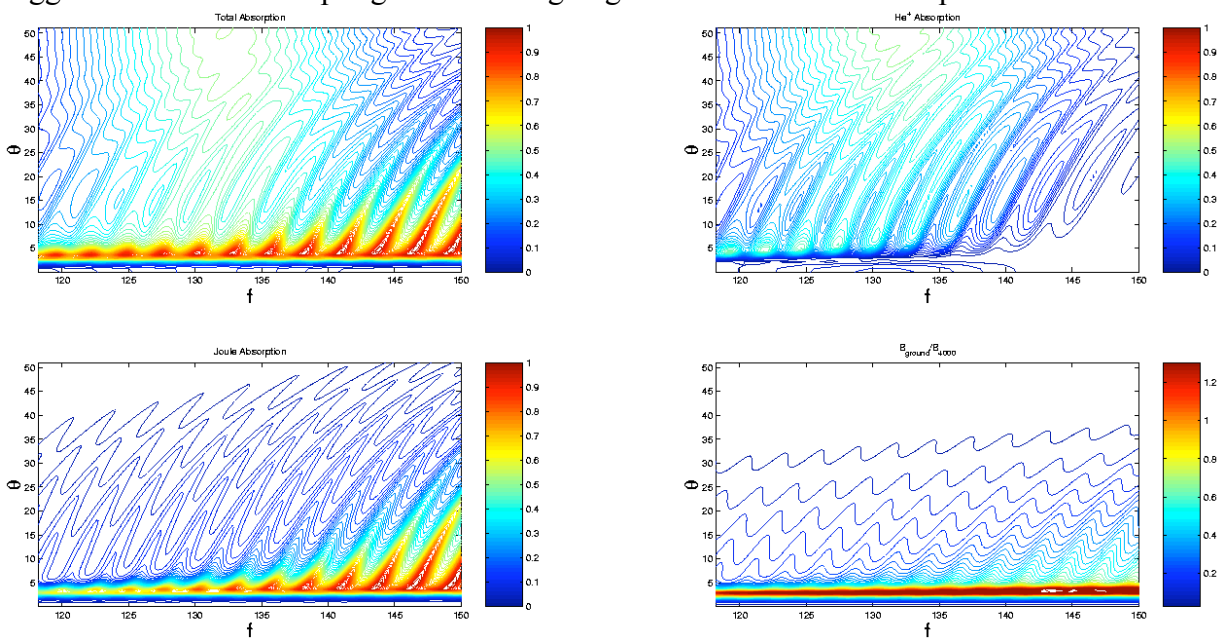

Figure 5. Wave absorption as a function of frequency and angle, θ, between the wavevector and magnetic field of the wave at the satellite location (4000 km). There is clearly a structure in the absorption coefficients with a frequency spacing around 2-3 Hz, which can affect the absorption coefficients by around 10-20 percent. The absorption structures increase in frequency with increasing angle suggesting coupling to the compressional wave.

The most obvious source of the modulations is coupling to a trapped compressional wave in the F-region. A trapped structure is admissible when a regular number of wavelengths fit into the F-region cavity of the Alfven velocity. The dispersion relation for the trapped wave is roughly $k_{\parallel} = \sqrt{(2\pi f_m/V_A)^2 - k_{\perp}^2} \approx 2\pi m/L_F$. The wavelength associated with each absorption maximum is fixed by the requirement that m wavelengths fit inside the F-region cavity. It can be seen why the mode appears in the F-region. Outside of the F-region, the Alfven velocity is large and the mode is nonpropagating. Inside the F-region where the density suddenly increases, the Alfven velocity decreases and the mode may

propagation. For each admissible mode, increasing $k_\perp$ (or θ) requires that the frequency shift upward as shown in Figure5. Moreover, for small $k_\perp$, the spacing of the high-m modes is basically v_A/L_F where L_F is the scale length of the F-region cavity. This number agrees well with the spacing of the modes at 2-3 Hz. In Figure 6 we test the scaling by decreasing the scale height L_F by a factor of two and increasing the density peak of the F-region by a factor of ten. The frequency spacing of the results for near parallel propagation shows an increase by a factor of two for the change in the scale height and a decrease by a factor of three in the spacing for the density increase. Both results are consistent with the scaling law $\Delta f = f_{m+1} - f_m \sim V_A/L_F$.

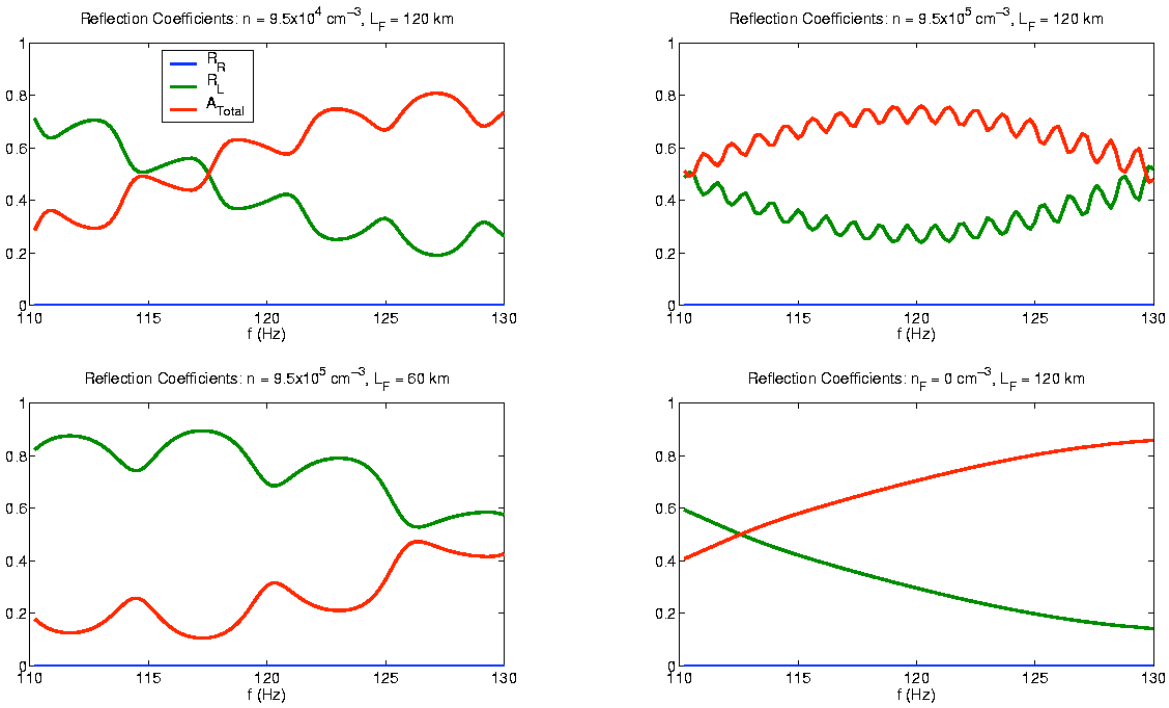

Figure 6. Absorption and reflection coefficients as a function of frequency for four different cases. The upper left panel shows a calculation using a typical auroral ionospheric model. The upper right panel shows coefficients when the F-region peak density is increased by a factor of 10. The decreased spacing is consistent with $\Delta f \sim 1/n^{1/2}$. The lower left panel shows the result when L_F is decreased by a factor of 2 consistent with the $\Delta f \sim 1/L_F$. The lower right panel shows the result when the F-region peak is removed (but the E-region peak remains). This final result clearly demonstrates that the modulations are due to the F-region, as the modulations no longer appear.

Waves and Background Plasma

The feedback between the waves and particles is an important topic because during disturbed magnetospheric configurations heavy ion outflows of ionospheric origin can dominate the energy

content of the plasma sheet. One method commonly employed when assessing wave-particle heating in the auroral region is based on quasilinear theory of ion heating where it is assumed that the observed wave spectrum at the satellite altitude accurately reflects the wave spectrum in the heating region below the spacecraft. However, this phenomenological approach does not take into account the possibility that the wave spectrum might be modified as the waves propagate down the field line into the ion heating region. Because wave propagation and ion heating efficiency depend heavily on the profile of the minor ion concentration, it is necessary to take the background plasma profiles into account when computing heating rates and determining ion outflows.

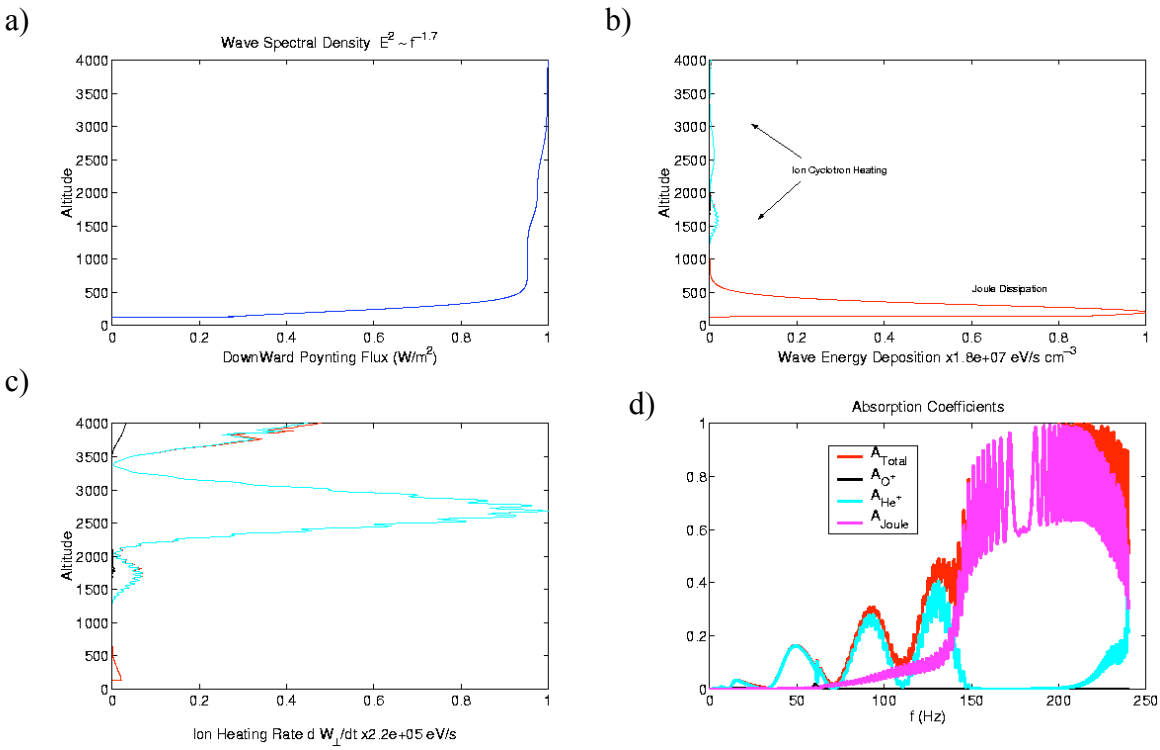

Figure 6. *Heating rates for a spectrum with spectral density which falls off as $f^{-1.7}$ with 5% helium and 5% oxygen and wave normal 60 degrees. Panel (a) shows Poynting flux, panel (b) shows wave energy deposition (energy/time) due to the waves, panel (c) shows ion heating rates obtained from the volume heating rate, and panel (d) shows the absorption coefficients as a function of frequency. Note that there is a one to one mapping between frequency and altitude. The peaks in absorption are related to wave reflection and interference.*

To illustrate how the heating rate depends on altitude, we take a wave spectral density that falls off with $f^{-1.7}$ at 5000km altitude. Auroral ion cyclotron waves with frequency below the local proton gyrofrequency typically are observed to have downward Poynting flux. As the waves propagate toward the ionosphere, Poynting flux is lost as indicated in Figure 6a where we have assumed a background concentration of 5% oxygen and 5% helium and wave-normal angle 60 degrees. From the loss of Poynting flux, we compute energy dissipated into ion cyclotron heating and Joule dissipation. Note that although the energy dissipated per volume is large in the ionosphere, the density of particles is also much larger and therefore Joule heating tends to be less

effective due to the large ionospheric sink of particles. Note that the heating rate shown in Figure 6c has maxima and minima which correspond to the maxima and minima in the absorption coefficients as a function of frequency (there is a one-to-one mapping of local ion cyclotron frequency and altitude). In Figure 7 we show the heating rates if there is 1% helium and 5% oxygen. Note that in this case, oxygen heating can be the dominant source of dissipation around 2000 km and 4000km while helium heating dominates at 3000km.

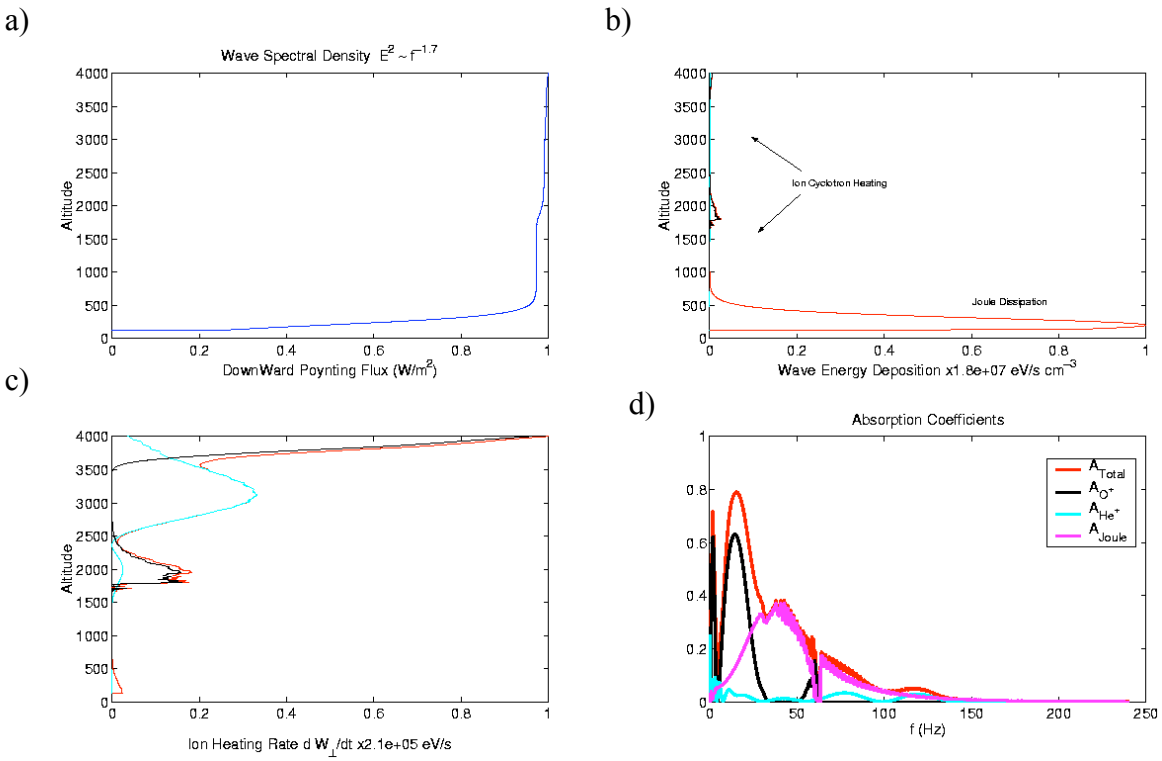

Figure 7. *Heating rates for a spectrum with spectral density which falls off as $f^{-1.7}$ with 1% helium and 5% oxygen and wave normal 60 degrees. Panel (a) shows Poynting flux, panel (b) shows wave energy deposition (energy/time) due to the waves, panel (c) shows ion heating rates obtained from the volume heating rate, and panel (d) shows the absorption coefficients as a function of frequency. Note in contrast to Figure 6 that significant oxygen heating occurs at 2000 and 4000 km and significant helium heating occurs at 3000 km. Thus, the heating rates depend sensitively on the background minor species profiles.*

When we use the heating rates obtained from the wave calculation with a Monte Carlo particle simulation of the ion distribution, we obtain the ion distribution shown in Figure 8. In this figure we show the ion distribution function obtained at ten altitudes ranging from the ionosphere to the auroral acceleration region. Note that the heating occurs in spurts with altitudes of strong heating followed by adiabatic heating. These ion distributions can be compared with distributions obtained from the more commonly employed heuristic heating rates which are shown in Figure 9. The major difference is the "self-similar" nature of the ions in Figure 9 which results from a balance in heating and adiabatic folding in contrast to the ions of Figure 8 which result from spurts of heating at favorable altitudes.

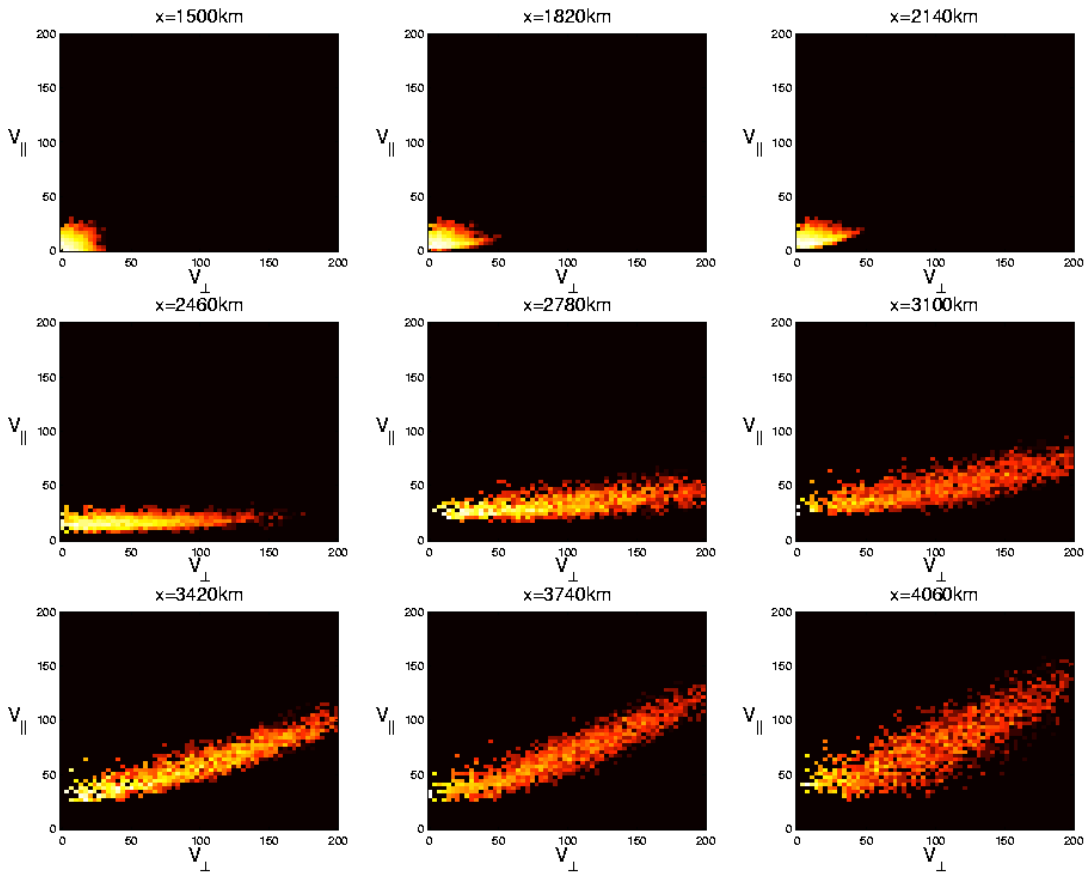

Figure 8. *Ion distribution, $f(v_{\perp},v_{||},z)$ as a function of altitude,z. Note that heating occurs in spurts followed by adiabatic conversion of perpendicular velocity to parallel velocity. Velocities are inicated in km/s.*

In Figure 10 we show the ion profiles obtained from our wave heating model. There are a number of items of note. Panel (a) shows that the energization peaks at around 200 eV with many particles accelerated to 1keV. Panel (b) shows the background density for the minor species consistent with the ion heating coefficient. Note, that this background density is not the same as the background density assumed in the wave propagation code. The reduced density in this case would allow waves to penetrate to lower altitude and pull more ions out of the ionosphere. The feedback should eventually shut off when the density falls low enough (around

1% for helium) where it may be possible to reach a steady state between the wave heating and background profiles. What this result suggests is that the waves penetrate into the topside ionosphere and start evaporating the ions there. As the evaporation carves away the minor ions in the topside ionosphere (energizing them to magnetospheric energies) the waves can propagate deeper and pull more ions out of the ionsphere until a steady state is reached. A future goal of this work is to examine the feedback of the density on the wave propagation model and to iterate to determine if there is a steady state profile and if not whether there is a limit cycle. Panels (c) and (d) show the pitch angle and energy as a function of altitude. Notice that the pitch angle has a kink which corresponds to the spurts of heating. In comparison, the heuristic heating rate gives roughly the same energies, but the background ion profile is different (it is smooth without steps). Note that

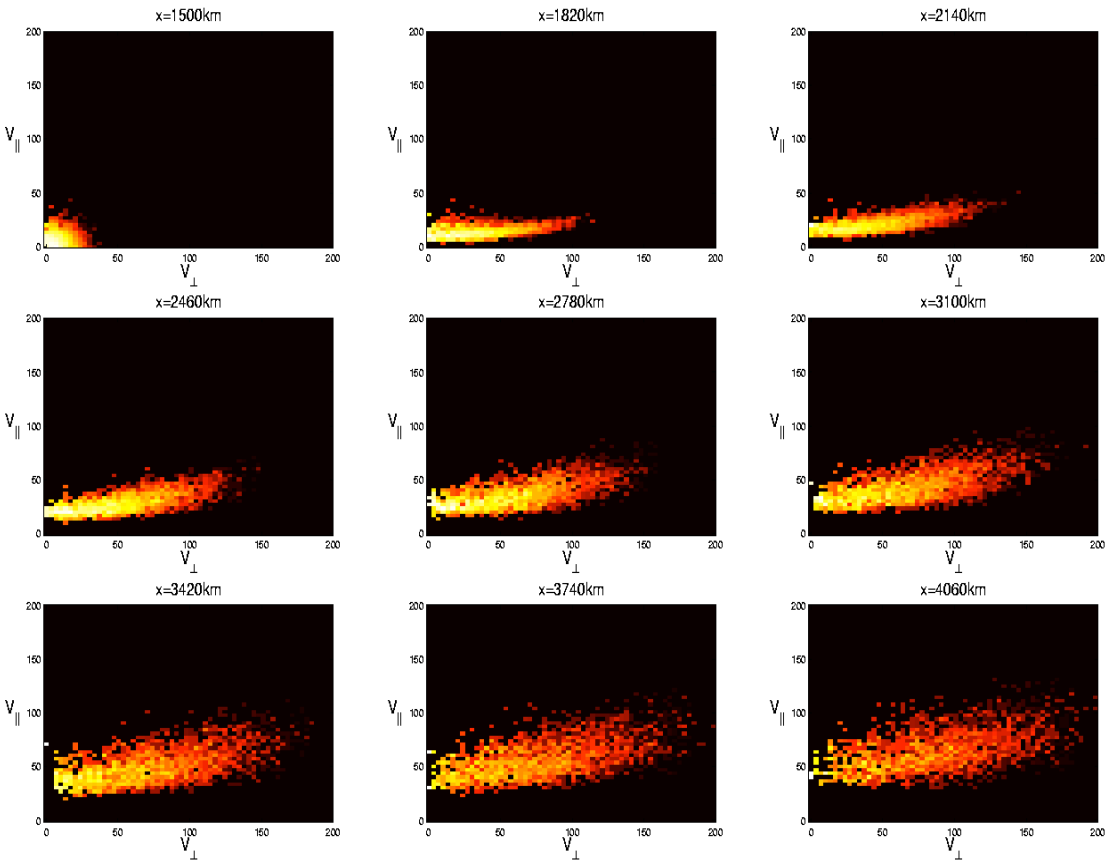

Figure 8. *Ion distribution, $f(v_{\perp},v_{||},z)$ as a function of altitude,z. Note that heating occurs in spurts followed by adiabatic conversion of perpendicular velocity to parallel velocity. Velocities are inicated in km/s.*

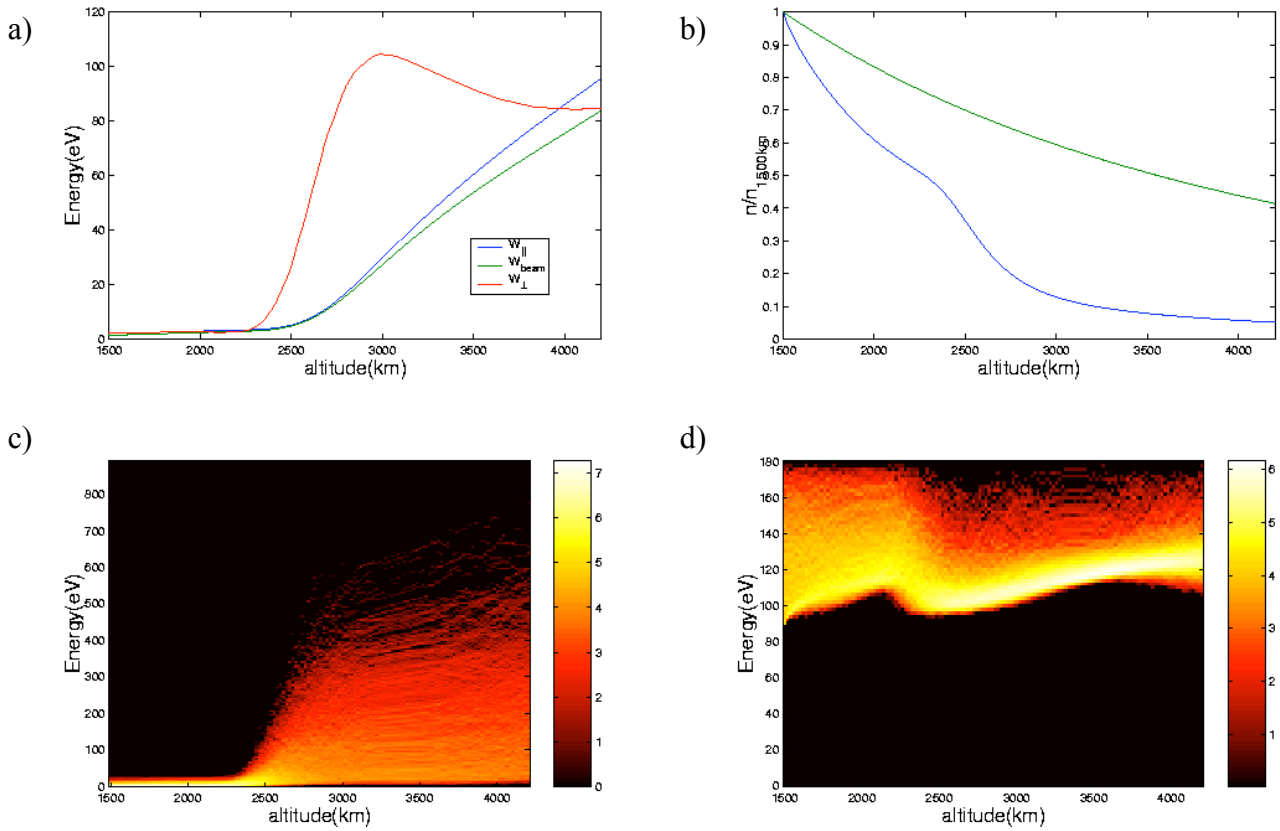

Figure 9. *Ion profiles obtained using the wave propagation model to obtain the ion heating rates. Panel (a) shows the energy as a function of altitude, panal (b) shows minor species density as a function of altitude, panel (c) shows energy as a function of altiude for the distribution and panel (d) shows the pitch angle as a function of altitude. In panel (b) the green line indicates the density falloff in the absence of ion heating with conservation of adiabatic moment (results because B decreases). Note that the waves carve out additional particles bringing them to higher altitude. The carving occurs in steps due to the peaks in ion heating rate as a function of altitude. The kink in the pitch angle (d) occurs because there is a spurt of heating (which brings the pitch angle closer to 90 degrees. Changing the minor species density significantly modifies this picture, therefore it will be necessary to solve the problem iteratively.*

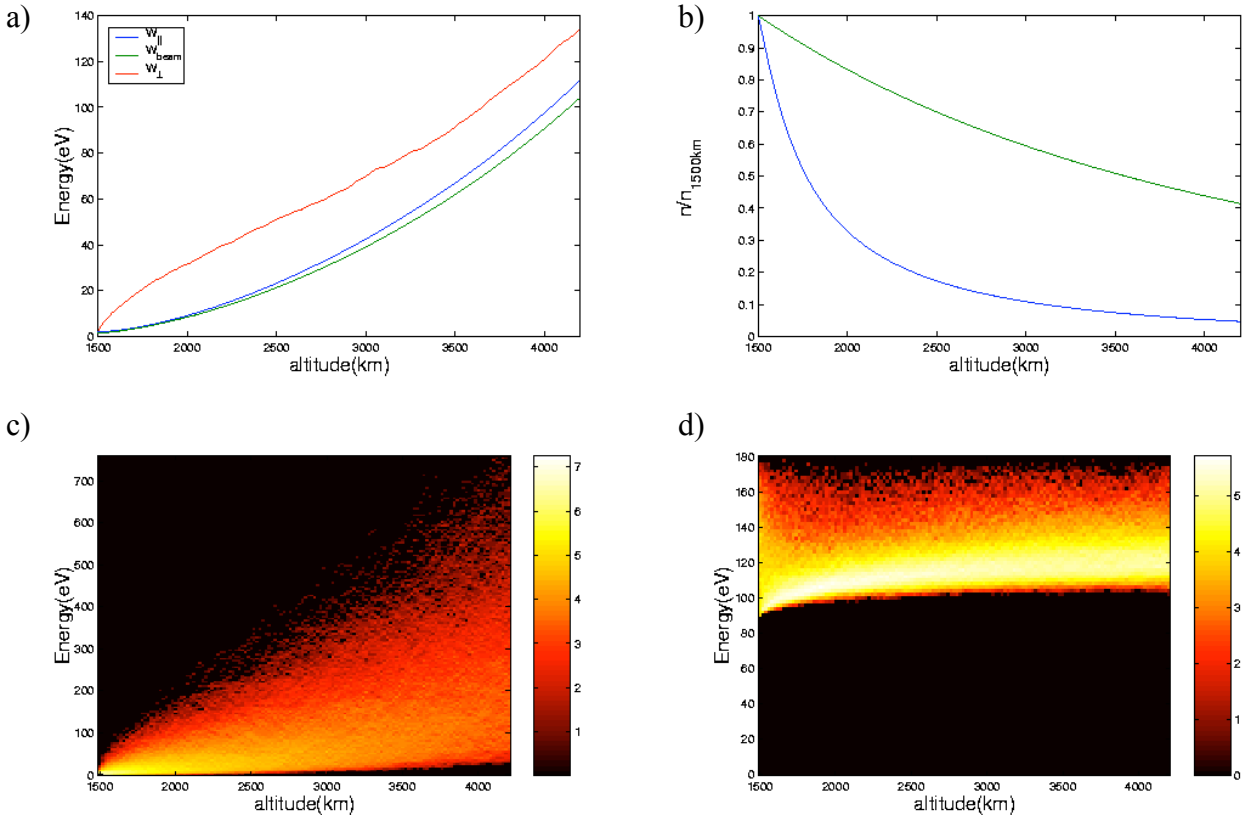

Figure 10. *Ion profiles obtained using heuristic ion heating rates based on the same spectrum as used in Figure 9.. Panel (a) shows the energy as a function of altitude, panal (b) shows minor species density as a function of altitude, panel (c) shows energy as a function of altiude for the distribution and panel (d) shows the pitch angle as a function of altitude. As in Figure 9 the density is carved out, but not in steps. These results do not depend on minor species concentrations as the theory does not account for wave propagation but assumes a ubiquitous spectrum along the length of the field line sharing the same spectral features.*

Self=Consistent Coupling Model

It is of interest to couple the wave propagation code with the Monte Carlo simulation code to describe ion outflows given a heating rate. We have combined these two codes together in an iterative way to obtain quasi-steady state ion profiles. The procedure is as follows: (a) we prescribe a wave spectrum at satellite altitudes and an initial plasma profile; (b) we compute the linear ion cyclotron wave solutions based on the spectrum (boundary condition) and plasma profile; (c) we compute the ion heating rate as a function of altitude based on the wave absorption computed from the wave code; (d) we perform Monte Carlo simulations of all ion species using the heating rate for each species to obtain distribution at each altitude; (e) we obtain the ion density profile and energy moments from the Monte Carlo simulation by integrating over the velocity space distribution function at each altitude; (f) we modify the ionospheric/magnetospheric plasma profiles; (g) we iterate (b)-(f) until the density profiles become stationary.

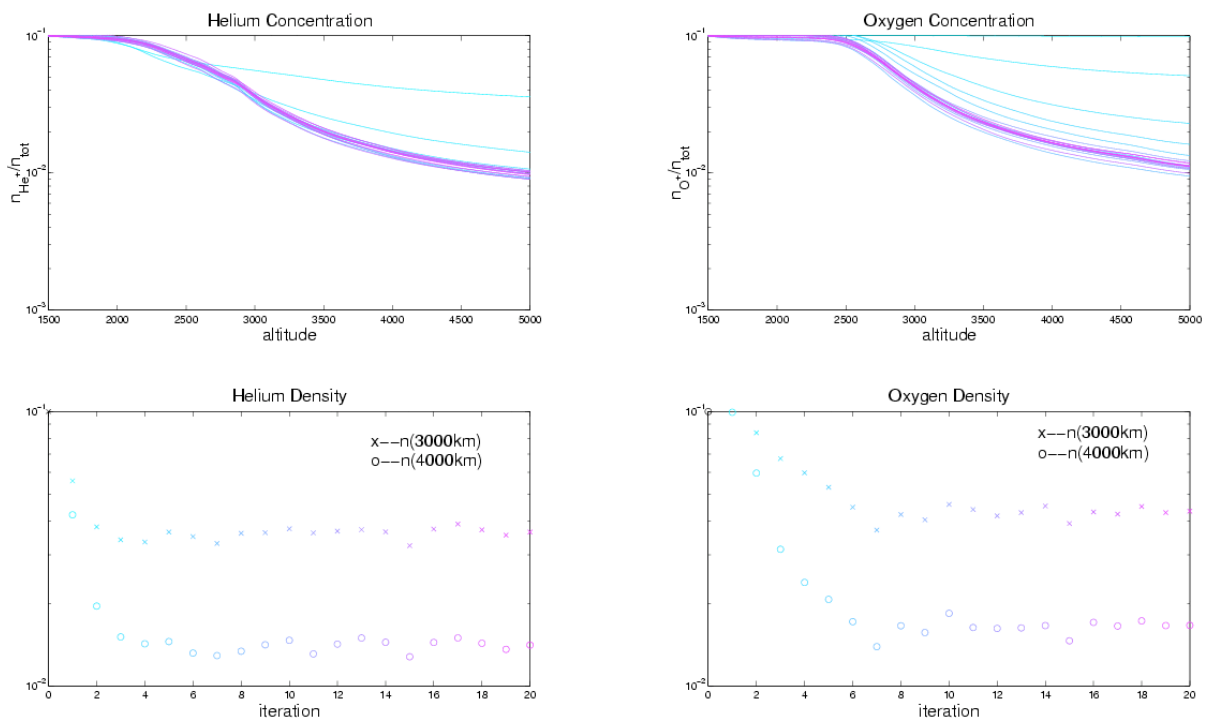

Figure 1. Convergence of the iterative scheme. Panels (a) and (b) show the helium and oxygen concentrations as a function of altitude for 20 iterations. Panels (c) and (d) show the convergence of the concentrations at 3000 km and 4000 km. Note the rapid convergence of the density profiles within 8 iterations.

This procedure is illustrated in Figure 1, which shows the relaxation of the plasma profiles as a function of iteration for a typical calculation. Panels (a) and (b) show the Helium and Oxygen fractional profiles as a function of altitude for 20 iterations. Panels (c) and (d) show the convergence of the density at 3000 km and 4000 km as a function of iteration number. In the absence of heating all ion species conserve adiabatic invariant

and move upward converting perpendicular to parallel energy. Ion heating increases the perpendicular energy and thus the parallel energy. Conservation of particle flux requires that $nv_{||}/B$ remains constant along a field line. Therefore, because the parallel velocity moment is increased by ion heating, the density is depleted leading to a decreased density. The density decreases until the ion heating rate due to waves comes into steady state with the ion outflows. It should be noted that the helium is first depleted before oxygen heating becomes important. This result occurs because oxygen heating is most efficient with lower helium concentrations. It is therefore necessary to first lower the helium concentration before oxygen can efficiently outflow. It is also apparent that helium is first heated at a lower altitude than oxygen. Although this is not a temporal simulation, it does suggest that ion outflows may occur as a two-stage process where one species is drawn out of the topside ionosphere and then allows the other species to also be drawn out.

The profiles for the helium and oxygen energy, density, and pitch angle are shown in Figures 2 and 3. For this calcuation, the waves are launched at 60 degrees to the magnetic field and density concentrations in the topside ionosphere below the heating region are taken as 5% helium and 1% oxygen. The perpendicular energy of the helium shows a large energy gain as a function of altitude and the heating occurs in several steps. The oxygen on the other hand is heated broadly in this altitude range with no apparent steps. The heating of oxygen is also much less dramatic than the helium heating. This result is somewhat surprising because the heuristic heating rate commonly used is proportional to $m^{\alpha-1}$ where α is the spectral index which is observed to be larger than 1. This being the case, one would expect preferential heating of oxygen. These results show the opposite. This dicrepency results because the waves deposit energy efficiently to helium in our calculation. The result is due to the propagation characteristics of the ion cyclotron wave and require a nonlocal treatment. Simply estimating heating rates below a satellite based on the spectrum observed at a satellite is not appropriate because different parts of the spectrum propagate differently and are absorbed differently.

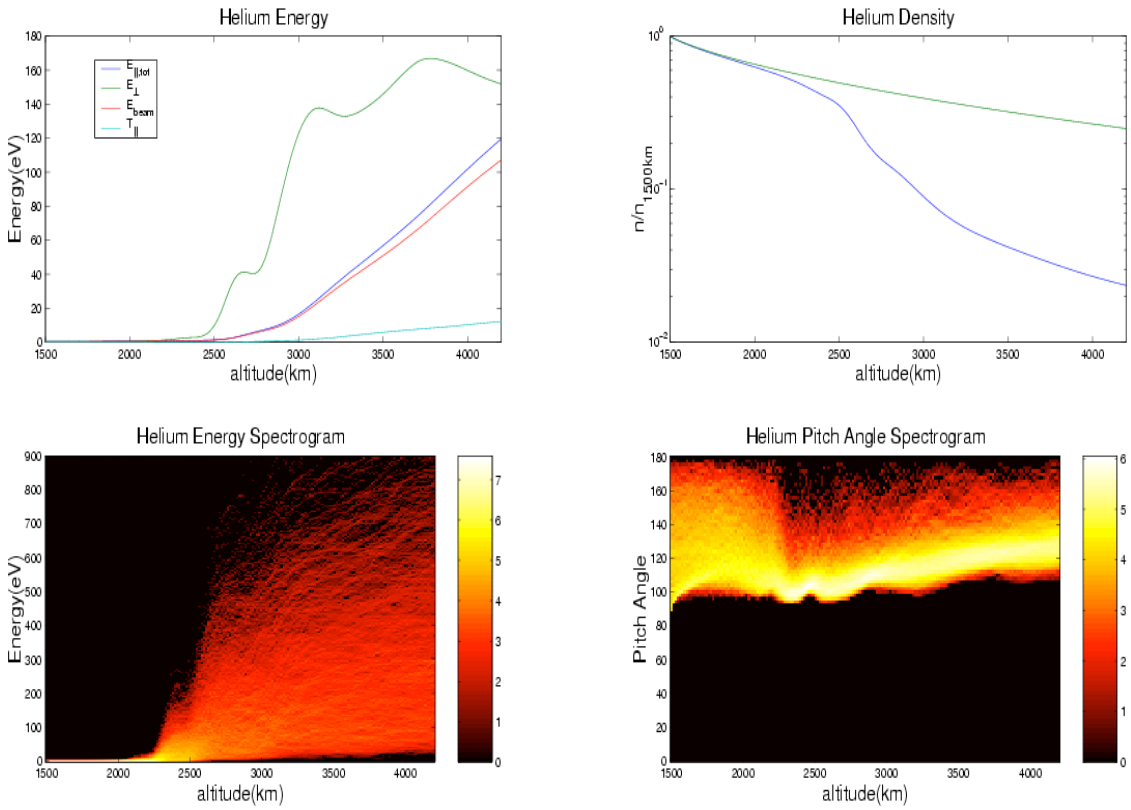

Figure 2. Helium energy and density profiles as a function of altitude. Note that the helium heating occurs in three sharp heating events. Using observed Poynting flux measurements, the helium is heated to 200eV.

The step-like accerlation of helium is also interesting. This accerlation results when wave interference affects the wave absorption at the resonance. As the waves reflect off the ionosphere they interfere with the downcoming waves leading to interference patterns. When the interference occurs near the location where the wave resonates with ions, there is little heating. When there is constructive interference at the resonance there is strong absorption of wave energy. For the wave structure, there are three such maxima in the range of the calculation.

The heating rates are computed from the wave calculations and are presented in Figure 4 where we show the downward Poynting flux, wave energy deposition, and ion heating rates for oxygen and helium. Most of the Poynting flux is lost at lowest altitude in the ionosphere. However, the ionosphere is such a large reservoir that not much energy is absorbed per particle. At higher altitude most of the energy is absorbed near the helium resonance. The helium heating rate shown in the lower left hand panel in blue has three peaks in accordance with the energy profiles shown in Figure 2. On the other hand, the oxygen heating rate does not vary so much over this altitude range. The reason that the variation is not as significant is because oxygen absorbs energy from lower frequency waves as its resonance is smaller than helium by a factor of 16. Higher frequency waves

at this altitude have much shorter wavelength and therefore, the spacing of the interference patterns for helium is much more pronounced.

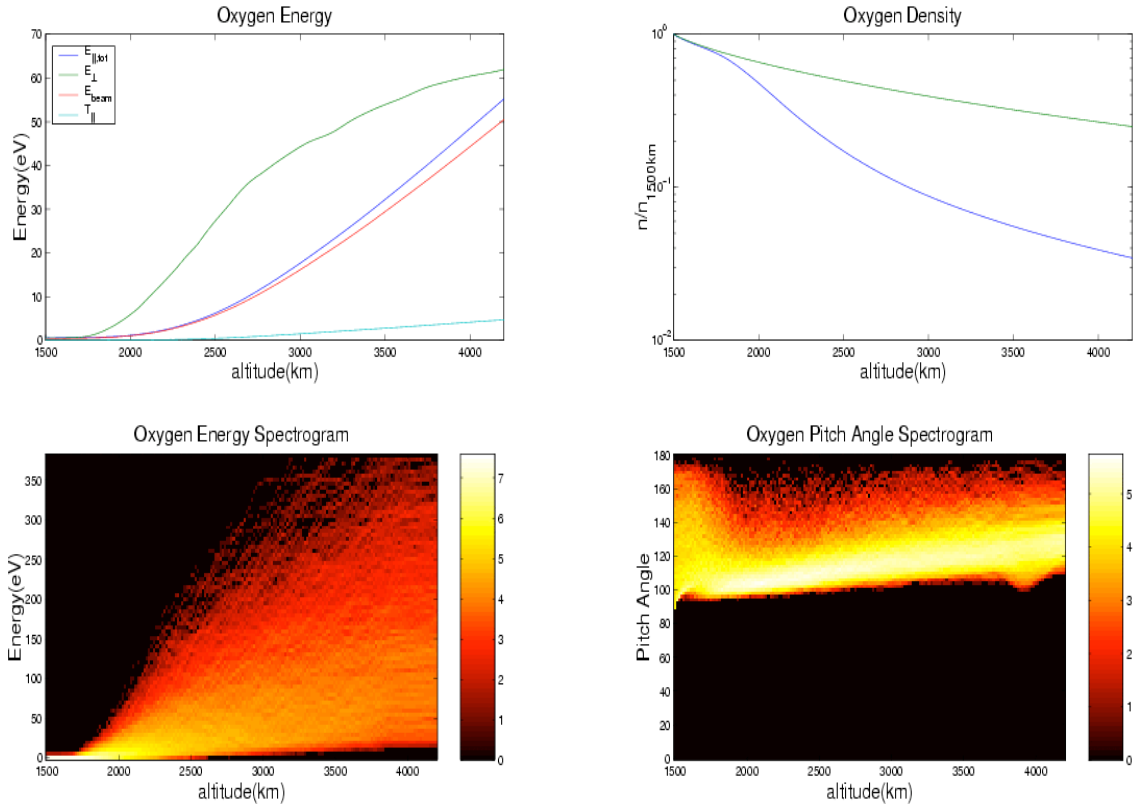

Figure 3. Oxygen energy and density profiles as a function of altitude. Note that the oxygen heating occurs over a broad range of altitude. Using observed Poynting flux measurements, the oxygen is heated to 60eV.

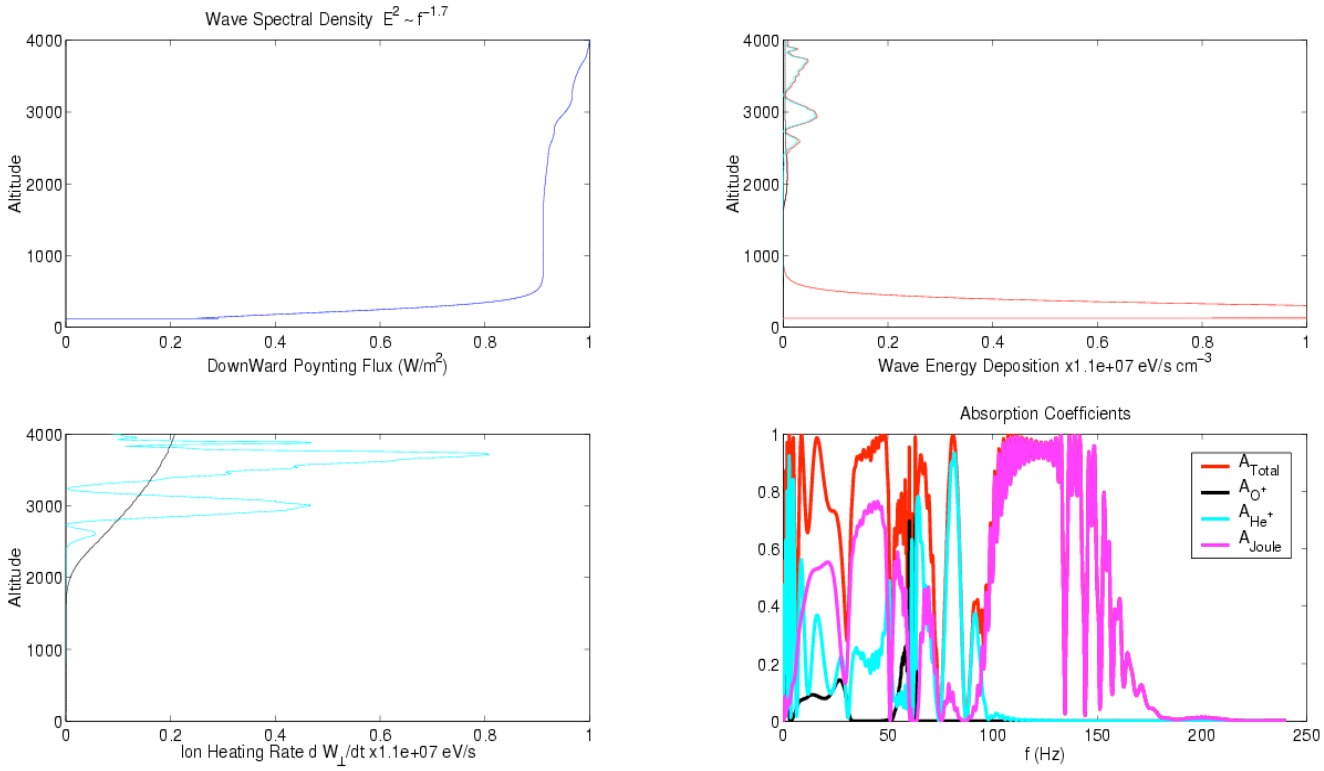

Figure 4. Poynting flux, wave energy dissipation, ion heating rate and absorption coefficients as a function of altitude. In the lower left hand panel, it is clear that the helium heating rate (shown in blue) has much more spatial variation than the oxygen heating rate (shown in black) and explains the multistep heating process.

These results are the first calculation that considers the nonlocal nature of the wave propagation and dissipation in obtaining ion profiles in the auroral region. Other results that are based on heuristic models while providing estimates of ion heating consistent with observations have missed some important physics. One important piece of physics is the result that nature of the wave propagation can completely change the density profiles and outflow. The results are sensitive to the nature of the instability and wave spectrum at the satellite as well as to various ionospheric processes that determine the relative ion densities in the topside ionosphere. In constructing feedback models for large scale simluations it is necessary to understand to some extent the instability mechanisms be they field aligned currents or velocity shear structure. It is also necessary to know the nature of the ion densities in the topside ionosphere. Moreover, it is also necessary to have a good ionospheric model because much of the wave absorption occurs after reflection of the ion cyclotron wave and the reflection depends sensitively on the ionospheric profiles. There are also some dynamical features that may also be important. For example, when considering oxygen outflows, it is important to keep in mind that helium plays a key role in determining how much oxygen can be heated because helium itself affects the propagation and absorption of the waves responsible for oxygen heating. Finally, observations commonly show that helium is more strongly heated than oxygen in the presence of EMIC waves. Although this finding is inconsistent with a heuristic model where the heating rate favors oxygen heating, it is consistent with our findings that

indicate that helium can be heated preferentially due to the dependence of wave absorption and propagation on wave frequency.

Summary of New Results:

1. We solved the wave equations for electromagnetic ion cyclotron waves propagating from the auroral acceleration region with downward Poynting flux taking into account minor ion species and a collisional ionosphere. We found both ion cyclotron and collisional absorption of the waves were important. One important consequence of this work was that we explained how the ion cyclotron waves could reach ionospheric altitudes and/or the ground if they were generated in the auroral acceleration region. Ray tracing results were not adequate to address this issue. The work serves as a motivation for setting up an array of higher frequency magnetometers which could be used to monitor EMIC waves and their sources in the auroral acceleration region.

2. We examined the strong dependence of wave absorption on the fraction of minor ions, frequency, and wave normal angle. We found two modulations of the absorption which appeared to be frequency dependent. The large scale modulation appears to be related to interference of upgoing and downgoing waves and does not appear in the case when the the ionospheric reflection is removed. Interference leads to minima in wave amplitude which minimize the absorption when they correspond to the resonance location. Changes in the frequency stretch the wavelength and shift the position of the minima. The small scale modulations are due to wave interaction with the F region of the ionosphere. There is coupling to a compressional wave in the F-region which produces modulations as in the case of the Alfven resonator.

3. We have explored the small scale variation of the absorption coefficients that result from coupling to a comrpessional wave in the F-region. By using different ionospheric profiles we are able to estimate the small scale variation of the absorption coefficients and how they depend on key parameters. The results demonstrate that the coupling results when wave energy is transferred to a trapped compressional wave in the F-region.

4. We obtained heating rates for a typical model for the wave spectrum at satellite altitudes using the wave propagation code. The heating rate was used in a Monte Carlo distribution of the ions and compared with the ion distribution obtained from the commonly employed heuristic heating rate. We found several items of note.

    a. First, the wave propagation model gives heating rates that depend on the minor ion profile, so we expect that the minor ion profile will adjust to balance the source (topside ionospheric density), heating and loss of the ions. This process could be important in the development of ion outflows and possibly lead to a steady state profile which balances wave heating, propagation, and background plasma profiles.

b. Second, the wave propagation model suggests that heating occurs in spurts and that there may be steps in the density and pitch angle profiles in the topside ionosphere.
c. Because the background ion density is modified by the waves, it is necessary to obtain a steady state plasma profile iteratively or search for a limit cycle if a steady state profile cannot be found. The development of the steady state could be related to relative concentrations of heavy ions that populate the plasma sheet during active times.

5. We have coupled together our wave propagation code and a Monte Carlo simulation using an iterative technique to obtain quasi-steady state self-consistent solutions for ion outflows given an observed power spectrum at satellite altitudes. This is the first work that has properly computed the ion outflows consistently with the observed wave spectrum accounting for wave propagation. The method is numerically stable and converges rapidly.

6. Based on this self-constent treatment we have discovered the nature of the wave propagation can completely change the density profiles and outflow. The results are sensitive to the nature of the instability and wave spectrum at the satellite as well as to various ionospheric processes that determine the relative ion densities in the topside ionosphere. These results imply that in constructing feedback models for large scale simluations it is necessary to understand to some extent the instability mechanisms be they field aligned currents or velocity shear structure. It is also necessary to know the nature of the ion densities in the topside ionosphere.

7. The convergence of our model also implies that some features would also be important for a dynamical simulation of ion outflows. For example, when considering oxygen outflows, it is important to keep in mind that helium plays a key role in determining how much oxygen can be heated because helium itself affects the propagation and absorption of the waves responsible for oxygen heating. It would appear that helium in many cases would first be drawn out prior to the appearance of oxygen outflows.

8. Observations commonly show that helium is more strongly heated than oxygen in the presence of EMIC waves. Although this finding is inconsistent with a heuristic model where the heating rate favors oxygen heating, it is consistent with our findings that indicate that helium can be heated preferentially due to the dependence of wave absorption and propagation on wave frequency.